

## Research Paper

Sensitization of melanoma cells to alkylating agent-induced DNA damage and cell death via orchestrating oxidative stress and IKK $\beta$  inhibition

Anfernee Kai-Wing Tse<sup>1,\*</sup>, Ying-Jie Chen<sup>1</sup>, Xiu-Qiong Fu, Tao Su, Ting Li, Hui Guo, Pei-Li Zhu, Hiu-Yee Kwan, Brian Chi-Yan Cheng, Hui-Hui Cao, Sally Kin-Wah Lee, Wang-Fun Fong, Zhi-Ling Yu\*

Center for Cancer and Inflammation Research, School of Chinese Medicine, Hong Kong Baptist University, Kowloon Tong, Hong Kong

## ARTICLE INFO

## Keywords:

Melanoma  
Reactive oxygen species  
IKK $\beta$   
Nitrosourea

## ABSTRACT

Nitrosourea represents one of the most active classes of chemotherapeutic alkylating agents for metastatic melanoma. Treatment with nitrosoureas caused severe systemic side effects which hamper its clinical use. Here, we provide pharmacological evidence that reactive oxygen species (ROS) induction and IKK $\beta$  inhibition cooperatively enhance nitrosourea-induced cytotoxicity in melanoma cells. We identified SC-514 as a ROS-inducing IKK $\beta$  inhibitor which enhanced the function of nitrosoureas. Elevated ROS level results in increased DNA crosslink efficiency triggered by nitrosoureas and IKK $\beta$  inhibition enhances DNA damage signals and sensitizes nitrosourea-induced cell death. Using xenograft mouse model, we confirm that ROS-inducing IKK $\beta$  inhibitor cooperates with nitrosourea to reduce tumor size and malignancy in vivo. Taken together, our results illustrate a new direction in nitrosourea treatment, and reveal that the combination of ROS-inducing IKK $\beta$  inhibitors with nitrosoureas can be potentially exploited for melanoma therapy.

## 1. Introduction

Malignant melanoma is a highly aggressive and treatment-resistant cancer, with increasing incidence and high mortality rates world-wide. The long term survival rate for patients with metastatic melanoma is only 5% [1]. Several therapeutic regimens such as vemurafenib/dabrafenib (targeting the BRAF V600E mutation), trametinib (targeting MEK), ipilimumab (targeting CTLA-4), and pembrolizumab and nivolumab (antibodies targeting programmed cell death 1) have resulted in an improved overall survival [2,3]. However, the above mentioned regimens are not suitable for the whole patient group due to the toxicity, lack of the V600E mutation and development of resistance, low response rate and other treatment strategies are therefore still required [2,3].

Alkylating agents are a class of anti-cancer chemotherapy drugs that bind to DNA and prevent proper DNA replication [4]. The monofunctional alkylating agents dacarbazine (DTIC) and temozolomide (TMZ) are approved in USA and frequently used for the treatment of melanoma for first-line therapy, but for most patients DTIC and TMZ treatment fails [5,6]. Due to the inherent drug-resistant char-

acteristic of this disease, chemotherapy by TMZ is an ineffective mean of treating malignant melanoma. The reasons for the chemoresistant phenotype in human melanoma are not well understood and are probably multifactorial [5].

Fotemustine is a nitrosourea alkylating agent approved in Europe, particularly in France and Italy, for use in the treatment of metastatic melanoma and gliomas [5,7]. The mechanism of action of fotemustine involves the induction of DNA interstrand cross-linking, which then leads to improper DNA replication and cell death [8,9]. Fotemustine is active in the treatment of melanoma brain metastases because it is able to cross the blood–brain barrier [10,11]. Fotemustine provides a better survival rate compared with DTIC for melanoma patients [12]. Nitrosourea alkylating agents are toxic to both cancer and normal cells, leading to damage in frequently dividing cells, as those in the gastrointestinal tract, bone marrow, testicles and ovaries, which can cause loss of fertility [8]. Nitrosourea alkylating agents also induce side effects consisted of headache, nuchal stiffness, vomiting, motor weakness, cranial nerve palsy, abnormal respiration and arrhythmia [13]. Moreover, there are serious side effects associated with fotemustine including myelosuppression, leucopenia, thrombocytopenia and toxic

*Abbreviations:* BRAF, serine/threonine-protein kinase B-Raf; ICL, DNA interstrand crosslink; IKK $\beta$ , Inhibitor of nuclear factor kappa-B kinase subunit beta; NAC, N-acetyl cysteine; NF- $\kappa$ B, Nuclear factor kappa B; ROS, Reactive oxygen species

\* Corresponding authors.

E-mail addresses: [anfernee@hkbu.edu.hk](mailto:anfernee@hkbu.edu.hk) (A.K.-W. Tse), [zlyu@hkbu.edu.hk](mailto:zlyu@hkbu.edu.hk) (Z.-L. Yu).

<sup>1</sup> These authors contributed equally to this work.

<http://dx.doi.org/10.1016/j.redox.2017.01.010>

Received 29 November 2016; Received in revised form 11 January 2017; Accepted 11 January 2017

Available online 12 January 2017

2213-2317/ © 2017 The Authors. Published by Elsevier B.V.

This is an open access article under the CC BY-NC-ND license (<http://creativecommons.org/licenses/by-nc-nd/4.0/>).

encephalopathy [7,14]. One approach to overcome these problems is to introduce a second chemical that enhances the cytotoxic effects of alkylating agents and allows the use of the inducers at lower and non-toxic doses.

The I $\kappa$ B kinase (IKK) enzyme complex is responsible for I $\kappa$ B phosphorylation which is essential for NF- $\kappa$ B signaling. Upon stimulation, the so-called canonical or classical pathway is activated, leading to the activation of IKK complex. Activated IKK $\alpha$  and/or IKK $\beta$  phosphorylate I $\kappa$ B $\alpha$  at S-32 and S-36. This causes I $\kappa$ B $\alpha$  ubiquitination and degradation by the 26 S proteasome, thereby, allowing NF- $\kappa$ B to translocate into the nucleus to regulate NF- $\kappa$ B target genes [15]. A growing body of evidence suggests that IKK $\beta$  may be a cancer treatment target in enhancing the cytotoxic effects by anti-cancer drugs, because several novel NF $\kappa$ B-independent functions of IKK $\beta$  have been identified recently, including promotion of DNA double strand break repair to promote cell survival and increase tumor cell resistance to ionizing radiation and chemotherapy [16–18]. However, no systemic study has been performed to review the potential synergistic action of IKK $\beta$  inhibitors on anti-cancer alkylating agents.

Reactive oxygen species (ROS) are chemically reactive molecules containing oxygen. High ROS production has been associated with significant decrease in antioxidant defense mechanisms leading to protein, lipid and DNA damage and subsequent disruption of cellular functions, leading to fatal lesions in cell that contribute to carcinogenesis [19]. On the other hand, ROS-inducing agents have been found to enhance the therapeutic effects of some anti-cancer agents. Previous study showed that tumor cell death induced by nitrosourea can be altered by the increase of ROS production [20], raising the possibility of using ROS-inducing compound as sensitizing agents for anti-cancer alkylating drugs.

Here, we investigate the potential therapeutic strategy for sensitizing the anti-tumor effect of nitrosourea alkylating agent using ROS-inducing IKK $\beta$  inhibitor.

## 2. Materials and methods

### 2.1. Reagents and antibodies

Antibodies against IKK $\beta$ , catalase, SOD1, p21, p27, p-Chk1(S345), Chk1, p-Chk2(T68), Chk2, p-H2AX(S139), H2AX, p-ATM(S1981), ATM, MGMT, PARP, Caspase-3, p-p53(S15), p53, survivin, XIAP, cIAP-1, cIAP-2, Mre11, Rad50, p95/NBS1, were purchased from Cell Signaling (Beverly, MA). Antibodies against Bak, Bcl-2, Bcl-xL, GAPDH, and actinin were purchased from Santa Cruz Biotechnology, Inc. Fotemustine and antibody against Flag (M2) was purchased from Sigma. 8-OHdG ELISA kit, mirin and SC-514 for in vivo experiment were purchased from Abcam. SC-514 for in vitro experiment, carmustine and lomustine were purchased from Enzo Life Sciences. PLX4032, BMS-345541, TPCA-1, LY-2409881, AZD3264, IKK-16 and PS-1145 were purchased from Selleckchem ML 120B dihydrochloride and PF184 were purchased from Tocris Bioscience. Crystal violet, propidium iodide (PI), N-acetyl-L-cysteine (NAC), temozolomide, 3-Amino-1,2,4-triazole (ATZ), hydrogen peroxide solution and 3-(4,5-Dimethyl-2-thiazolyl)-2,5-diphenyl-2H-tetrazolium bromide (MTT) were purchased from Sigma. 6-Carboxy-2',7'-dichlorofluorescein diacetate (DCF) was purchased from Thermo Scientific.

### 2.2. Cell cultures

IGR-1 cells were obtained from CLS Cell Lines Service GmbH. All the other melanoma cell lines were obtained from American Type Culture Collection. All cell lines were cultured in DMEM supplemented with 5% fetal calf serum, 100 units/ml penicillin, and 100 mg/ml streptomycin. Human dermal fibroblasts adult (HDFa) cells were obtained from Thermo Fisher Scientific and cultured with Medium 106 supplemented with Low Serum Growth Supplement Kit. All cell

lines were authenticated by genotyping, found to be mycoplasma free and typically used within 20 passages. BRAF inhibitor resistant clones were cultured in increasing concentrations of PLX4032 (0.1–1  $\mu$ M) and the resistant clones were maintained in 1  $\mu$ M PLX4032 thereafter.

### 2.3. Modified alkaline comet assay

The alkaline comet assay was used to detect fotemustine-induced DNA crosslinks in melanoma cells. Briefly, at 4 h after drug exposure, cells were harvested in ice cold PBS by scraping and the pellet was resuspended in ice-cold PBS. Cells were incubated with 50  $\mu$ M hydrogen peroxide to induce strand breaks for 10 min at 4  $^{\circ}$ C, centrifuged at 2000g for 5 min at 4  $^{\circ}$ C and resuspended in PBS. The comet assay was performed as then. Briefly, cell samples were added to an equal volume of 1% low melting point agarose and embedded on comet assay slide (Cell Biolabs, Inc). The slides were then incubated in lysis solution (2.5 N NaCl, 10 mM Tris, 100 mM EDTA, pH 10.5, 1% v/v Triton X-100) overnight at 4  $^{\circ}$ C in the dark. Slides were equilibrated in fresh electrophoresis buffer (50 mM NaOH, 1 mM EDTA, pH 12.5) and electrophoresed for 30 min at 0.6 V/cm in the dark. Following electrophoresis, slides were washed twice in neutralizing buffer (500 mM Tris, pH 7.5) and 5 min in distilled water and dried overnight. Next day, they were rehydrated 30 min with distilled water and stained 30 min with Vista Green DNA Dye (Cell Biolabs, Inc) at a 1:10000 dilution. The slides were finally illuminated with green light under fluorescence microscope (Leica), linked to a CCD camera. DNA migration was analyzed using the CaspLab software (<http://www.casp.of.pl>), by measuring 50 cells per slides and the data was expressed as percent of DNA in the comet tail (Tail DNA%).

### 2.4. In vitro DNA crosslink assay

The in vitro DNA cross-linking was measured using a modified DNA renaturation. Briefly, calf-thymus DNA (250  $\mu$ g/ml) was exposed to alkylating agents and/or H<sub>2</sub>O<sub>2</sub> in buffer (10 mM Tris-HCl, 1 mM EDTA, pH8.0), and incubated at 37  $^{\circ}$ C for 16 h. The mixture was removed and 0.1  $\mu$ g/ml Hoechst 33258 was added as the fluorescent probe, which binds selectively to double stranded DNA and generates intense fluorescence. Then each sample was unheated or heated at 98  $^{\circ}$ C for 5 min, and plunged into ice water for 5 min, and followed by incubation at room temperature for 5 min. The fluorescence was measured using a fluorescence microplate reader (EnVision<sup>®</sup>, PerkinElmer). The cross-linked fraction (CF) was described as  $CF = (E_a/E_b - C_a/C_b) / (1 - C_a/C_b)$ .  $E_a$  is the fluorescence of the experimental sample after heat/chill,  $E_b$  is the fluorescence of the experimental sample before heat/chill,  $C_a$  is the fluorescence of the control sample after heat/chill, and  $C_b$  is the control of the experimental sample before heat/chill.

### 2.5. Immunofluorescence

Melanoma cells were grown on 4-well chambered slides (SPL Life Sciences), fixed with 4% paraformaldehyde for 10 min, and permeabilized with 0.1% Triton X-100 for 5 min. After permeabilization, slides blocked in PBS/1% BSA for 1 h at 37  $^{\circ}$ C, and incubated overnight at 4  $^{\circ}$ C with the following primary antibodies: rabbit monoclonal  $\gamma$ H2AX (Ser-139), 1:1000 (Cell Signaling Technology). Secondary antibodies labeled with Alexa 488 (Abcam) were added at 1:1000, and slides were incubated at 37  $^{\circ}$ C for 1 h. Slides were mounted with Fluoroshield Mounting Medium With DAPI (Abcam). Images were acquired at room temperature with a Leica DMI3000 B microscope.

## 2.6. Construction of plasmids, transient transfection and luciferase activity assay

The NF- $\kappa$ B luciferase reporter (pNF- $\kappa$ B-Luc) was obtained from Clontech. MGMT full length expression constructs were synthesized by PCR using A375 total mRNA and subcloned into the pcDNA3-Flag tagged vector. The cDNA of IKK $\beta$ -WT and IKK $\beta$ -SS/EE, encoding wide type or constitutively active IKKs were generously supplied by Dr. Richard B. Gaynor (Department of Medicine, University of Texas Southwestern Medical Center, USA [21], and subcloned into the pcDNA3-Flag tagged vector. The pcDNA3-catalase-Flag tagged vector was constructed as described [22]. The plasmid transfection and luciferase assay were the same as described previously [23]. Firefly and renilla luciferase activities were assayed according to the manufacturer's protocol (Promega). Firefly luciferase activity was normalized to renilla luciferase activity in cell lysate and expressed as an average of three independent experiments.

## 2.7. Cytotoxicity assay and crystal violet staining

For crystal violet staining assay, cells ( $1 \times 10^4$ ) were seeded in 60 mm dishes, and then untreated or pretreated with SC-514 and/or fotemustine. Then, cells were formalin-fixed and stained with crystal violet. Cell numbers were measured as the optical density at 595 nm (OD595) of solubilized crystal violet from formalin-fixed cells. Cytotoxicity were also determined by the MTT reduction assay [24].

## 2.8. Western blot analysis

Whole-cell protein was prepared and analyzed by Western blotting as described previously [25].

## 2.9. Small interfering RNA (siRNA) treatment

Silencing of Catalase or SOD1 was achieved by transfecting siRNAs (Thermo Scientific) using Lipofectamine 2000 (Invitrogen) according to the manufacturer's recommendations. Gene silencing effect was evaluated by Western blot analysis.

## 2.10. Measurement of reactive oxygen species

Cells were plated in black 96-well plates and allowed to attach for 24 h. Then cells were loaded with fluorescent dyes, 6-Carboxy-2',7'-dichlorofluorescein diacetate (DCF-DA), and further stimulated with SC-514 and/or fotemustine. Fluorescence was measured using a fluorescence microplate reader (EnVision® Multilabel Reader, PerkinElmer) at indicated time point at 37 °C. For DCF fluorescence microscopy, G361 cells were seeded in 4-well cell culture slide chamber (SPL Life Sciences) and treated with 50  $\mu$ M SC-514 and/or NAC for 4 h. 10  $\mu$ M of DCF-DA were then loaded to cells, afterwards, the samples were rinsed twice with saline, fixed with 4% paraformaldehyde, and counter-stained with DAPI. Images were acquired at room temperature with a Leica DMI3000 B microscope.

## 2.11. Cell cycle analysis

For cell cycle analysis, cells were collected, washed, resuspended in cold PBS, fixed in 75% ethanol at -20 °C overnight, washed and resuspended in PBS with RNAase. Cellular DNA was stained with PI and cell samples were analyzed on a Becton Dickson flow cytometer (BD Biosciences, USA) using CELL Quest software (Verity Software House Inc., Topsham, ME).

## 2.12. Annexin V/PI assay

The indicator of cell death and apoptosis was detected by using

annexin V/PI binding kit (Abcam). Briefly, A375 and G361 cells were treated with SC-514 and/or fotemustine for 48 h. Then, cells were trypsinized, stained with annexin V/PI and then analyzed with flow cytometer.

## 2.13. In vivo xenograft melanoma model

Male nu/nu BALB/c mice (6 weeks old) were obtained from BioLASCO Taiwan (Taipei, Taiwan). The nude mice were maintained in individual ventilated cages in a specific animal handling room of Hong Kong Baptist University. All care and handling of animals were performed with the approval of the Government of The Hong Kong Special Administrative Region Department of Health. A375 or G361 ( $5 \times 10^6$ ) cells were resuspended in 0.1 ml PBS and inoculated subcutaneously into the backs of nude mice and allowed to grow for 7 days. After that, mice were randomly assigned to 4 groups (n=6 for each group) and treated by intraperitoneal injection with 200  $\mu$ l 30% PEG/5% Tween-80 solution as the vehicle control and 25 mg/kg SC-514 and/or 25 mg/kg fotemustine daily for 13–15 consecutive days. Body weight and tumor volume were measured every 3 days. Tumor volumes were determined by a caliper and calculated according to the following formula: (width<sup>2</sup>×length)/2. At the end of the experiment, mice were sacrificed and tumor xenografts were collected. Tumor tissues were stored at -80 °C for Western blot analysis.

## 2.14. Statistical analysis

Statistical analysis was performed using Origin 6.0 (Origin software). All data are expressed as mean  $\pm$  SD of 3 independent experiments. Statistical significance was determined using unpaired Student's t-test and a P value of less than 0.05 was considered statistically significant.

## 3. Results

### 3.1. Dual targeting of IKK $\beta$ and antioxidant enzyme sensitizes nitrosourea-induced melanoma cell death

Recently reports indicate that inhibition of IKK $\beta$  or induction of ROS could enhance cancer cell death induced by nitrosoureas [16,20]. However, the dual effect of IKK $\beta$  inhibition and ROS induction on nitrosourea-induced cell death is not known. To determine the dual effect of IKK $\beta$  inhibition and ROS induction, we treated human melanoma cell lines with IKK $\beta$  and/or antioxidant enzyme catalase siRNA together with fotemustine. A375 and G361 melanoma cell lines showed low sensitivity to fotemustine alone (Fig. 1, A and B). Individual knockdown of IKK $\beta$  or catalase led no or only slight enhancement in fotemustine-induced cytotoxicity. Interestingly, simultaneous treatment with IKK $\beta$  and catalase siRNA resulted in synergistic increases in growth inhibition induced by fotemustine in both A375 and G361 cells (Fig. 1, A and B). We also observed that simultaneous treatment with IKK $\beta$  and superoxide dismutase 1 (SOD1) siRNA resulted in increase in growth inhibition induced by fotemustine (Supplementary Fig. S1). These results indicate that IKK $\beta$  inhibition and ROS induction together, but not alone, could augment nitrosourea-induced melanoma cell death.

### 3.2. SC-514 is a ROS-inducing IKK $\beta$ inhibitor

On the basis of the findings above, we next explored the ROS-inducing properties of current specific IKK $\beta$  inhibitors. Nine specific IKK $\beta$  inhibitors (Fig. 2A) were screened for their capacity to alter ROS levels in cultured cells. All selected IKK $\beta$  inhibitors were able to show differential inhibitory effects on the intrinsic NF- $\kappa$ B activity, as evidenced by NF- $\kappa$ B luciferase assay (Fig. 2B). Next, we investigated whether these IKK $\beta$  inhibitors could alter ROS levels in melanoma

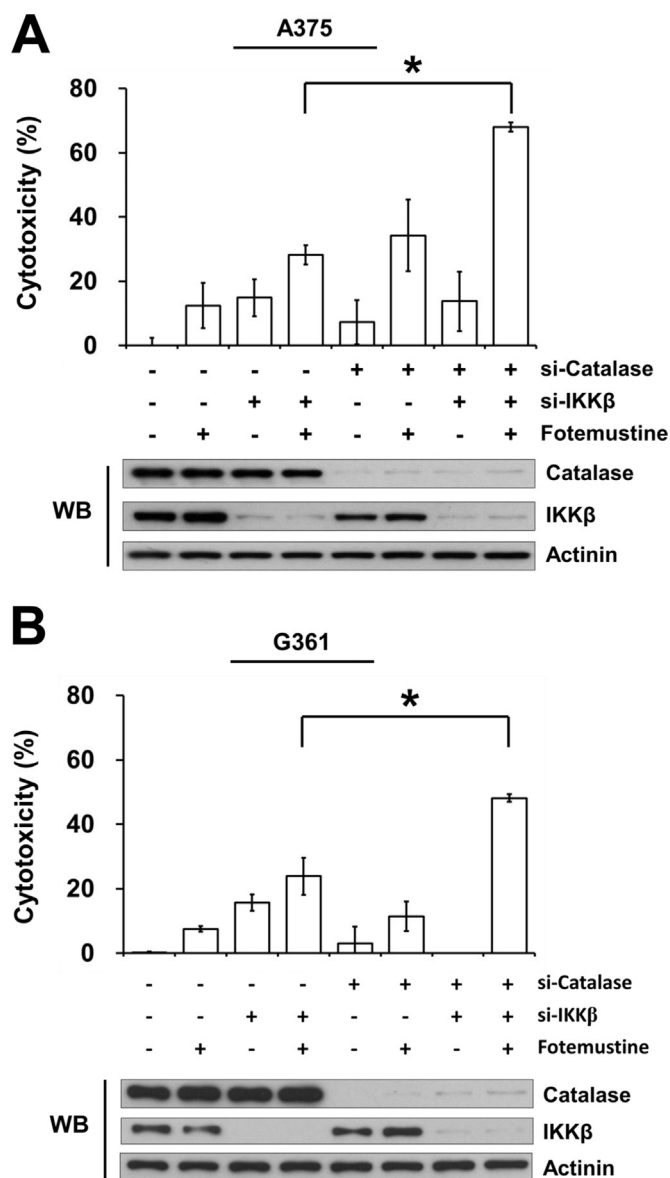


**Fig. 1.** Combining Catalase and IKK $\beta$  Inhibition Sensitizes Melanoma Cells to Nitrosourea Treatment. (A) After transfection with control, catalase and/or IKK $\beta$  siRNAs for 24 h, A375 cells were treated with vehicle or 50  $\mu$ M of fotemustine for an additional 48 h. Cell viability was then assessed. \*,  $p < 0.05$ . Western blot analysis of catalase and IKK $\beta$  after same treatment is also shown. (B) After transfection with catalase and/or IKK $\beta$  siRNAs for 24 h, G361 cells were treated with vehicle or 50  $\mu$ M of fotemustine for an additional 48 h. Cell viability was assessed by the MTT assay. \*,  $p < 0.05$ . Western blot analysis of catalase and IKK $\beta$  after same treatment is also shown.

cells. We found that among all compounds being tested, only SC-514 produced an increase in the endogenous ROS levels in G361 melanoma cells (Fig. 2C), and the increase in ROS levels was inhibited by antioxidant NAC co-treatment (Fig. 2D). We also observed that SC-514 induced ROS production in a consistent manner during 3 h treatment period (Fig. 2E). Moreover, SC-514 was able to induce ROS in all other melanoma cells being tested including A375, COLO829, Malme-3 M, Sk-MEL-5 and SK-MEL-28 cells (Supplementary Fig. S2), indicating that the ROS-inducing property of SC-514 was not cell-type specific.

### 3.3. SC-514 synergizes with nitrosoureas to kill melanoma cells

To evaluate whether the ROS-inducing IKK $\beta$  inhibitor increases the sensitivity of melanoma cells to nitrosourea, we first assessed the responses of melanoma cells to SC-514/fotemustine co-treatment.

Melanoma cell lines were treated with 50  $\mu$ M of SC-514 and fotemustine alone and in combination for 48 h and growth inhibition was assessed. As shown in Fig. 3A, co-treatment with SC-514 significantly enhanced fotemustine-induced cytotoxicity in all melanoma cell lines tested, suggesting that the enhancement effect of SC-514/fotemustine is not cell-type specific. Interestingly, no enhancement effect was observed in normal human adult dermal fibroblast cells (HDFa) (Fig. 3A).

To determine the long term growth inhibitory effects, we treated various melanoma cells with vehicle or SC-514 and /or fotemustine for 7 days. Under these conditions, cells treated with vehicle, SC-514 alone, or fotemustine alone remained viable and continued to grow (Fig. 3B). In contrast, the combination of SC-514 and fotemustine led to the elimination of viable cells, indicating that the fotemustine-sensitizing action of SC-514 significantly reduced long term cell survival.

Besides fotemustine, several other cytotoxic alkylating agents containing the lipophilic chloroethyl-nitrosourea group, such as carmustine and lomustine, were also used to treat melanoma [26]. To test whether SC-514 synergizes with other nitrosoureas, we tested the cell viability of SC-514 in combination with carmustine and lomustine. The addition of SC-514 to carmustine and lomustine exerted higher cytotoxicity compared with carmustine alone and lomustine alone (Fig. 3C), suggesting that the augmentation effect of SC-514 to nitrosoureas was not limited to fotemustine. On the other hand, SC-514 was not able to enhance the cytotoxic effect of the monofunctional alkylating temozolomide (Fig. 3C).

Activating V600E mutation in the BRAF oncogene was found in over half of the patients with advanced melanoma [27]. Inhibition of the oncogenic BRAF protein with the small molecule inhibitor PLX4032 (vemurafenib) has shown impressive initial responses in patients with BRAF mutant melanoma [28]. However, BRAF therapies for advanced melanoma are rarely curative, due to the rapid development of resistance, relapse and side effects [29]. To determine whether fotemustine-induced cell growth inhibition can be enhanced by SC-514 in BRAF inhibitor resistant cells, we generated BRAF mutant A375-R and G361-R melanoma cell clones that were less sensitive to the BRAF inhibitor PLX4032 than their respective parental cells. As presented in Fig. 3D, SC-514 was able to augment fotemustine-induced cytotoxicity in A375-R and G361-R cells. These data clearly demonstrate the enhancement ability of SC-514 on fotemustine in BRAF inhibitor resistant cells.

As described in Fig. 2C, SC-514 was the only IKK $\beta$  inhibitor that could induce ROS. We also investigated the possible enhancing effect from the combination of non-ROS-inducing IKK $\beta$  inhibitor and fotemustine together with knockdown or inhibition of antioxidant enzyme. We found that either knockdown of catalase or inhibition of catalase activity by catalase inhibitor aminotriazole (ATZ) was able to boost the enhancing ability of non-ROS-inducing IKK $\beta$  inhibitors BMS-345541 and PS-1145 to fotemustine-induced cell death (Fig. 3, E and F). This indicates that the induction of ROS by other ways or sources could also contribute to the enhancing effects.

### 3.4. SC-514/fotemustine combination induces concomitant DNA damage, cell cycle arrest and apoptosis in human melanoma cells

Fotemustine was found to induce either S or G2-M phase arrest in the cell cycle in melanoma cells [30]. To evaluate whether SC-514/fotemustine inhibits cell proliferation via the regulation of cell-cycle, cell-cycle analysis was carried out by flow cytometry. When melanoma cells exposed to SC-514/fotemustine for 24 h, increase of cells in G<sub>2</sub>-M phase was observed in A375 cells, while accumulation of S phase cells was observed in G361 cells (Fig. 4A). SC-514/fotemustine-mediated cell cycle arrest was associated with increase in cell cycle regulatory proteins p21, p27, p53 (Fig. 4B). SC-514/fotemustine combination remarkably induced phosphorylation of Chk1 at Ser345 in both A375

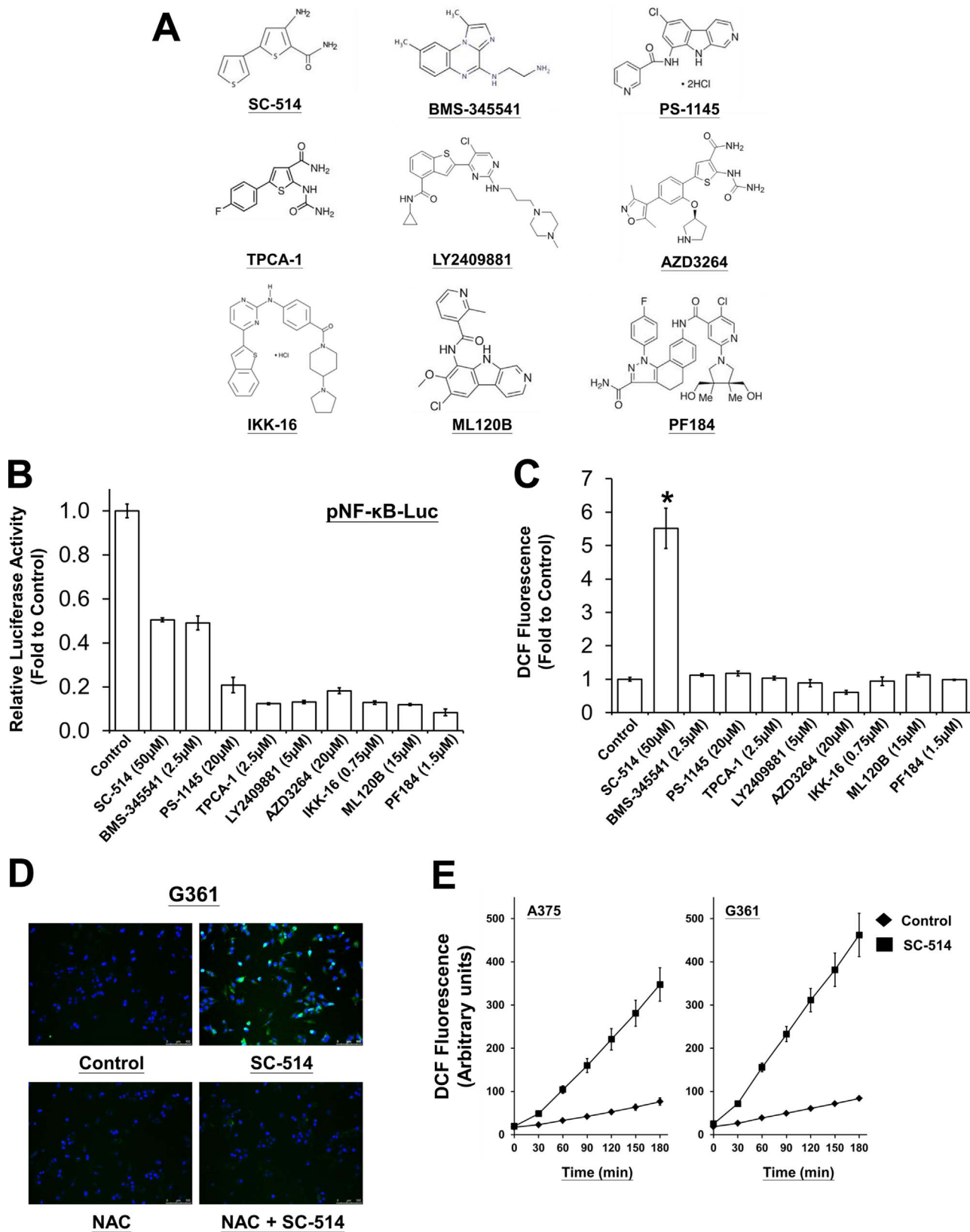


**Fig. 2.** SC-514 is a ROS-inducing IKK $\beta$  Inhibitor. (A) Chemical structure of nine IKK $\beta$  inhibitors. (B) Luciferase activity of G361 cells transfected with pNF- $\kappa$ B-Luc and treated with vehicle or indicated IKK $\beta$  inhibitors for 24 h. At least two independent experiments with triplicates revealed comparable results. (C) G361 cells were loaded with DCF (ROS probe) and further stimulated with vehicle or indicated IKK $\beta$  inhibitors for 3 h. Fluorescence was measured using a fluorescence microplate reader. \*,  $p < 0.05$  versus control. (D) Fluorescence microscopy images of DAPI and DCF stained G361 cells treated with 50  $\mu$ M SC-514 and/or 5 mM NAC for 4 h. (E) DCF fluorescence was measured in A375 and G361 melanoma cells treated with vehicle or 50  $\mu$ M of SC-514 at indicated time intervals.

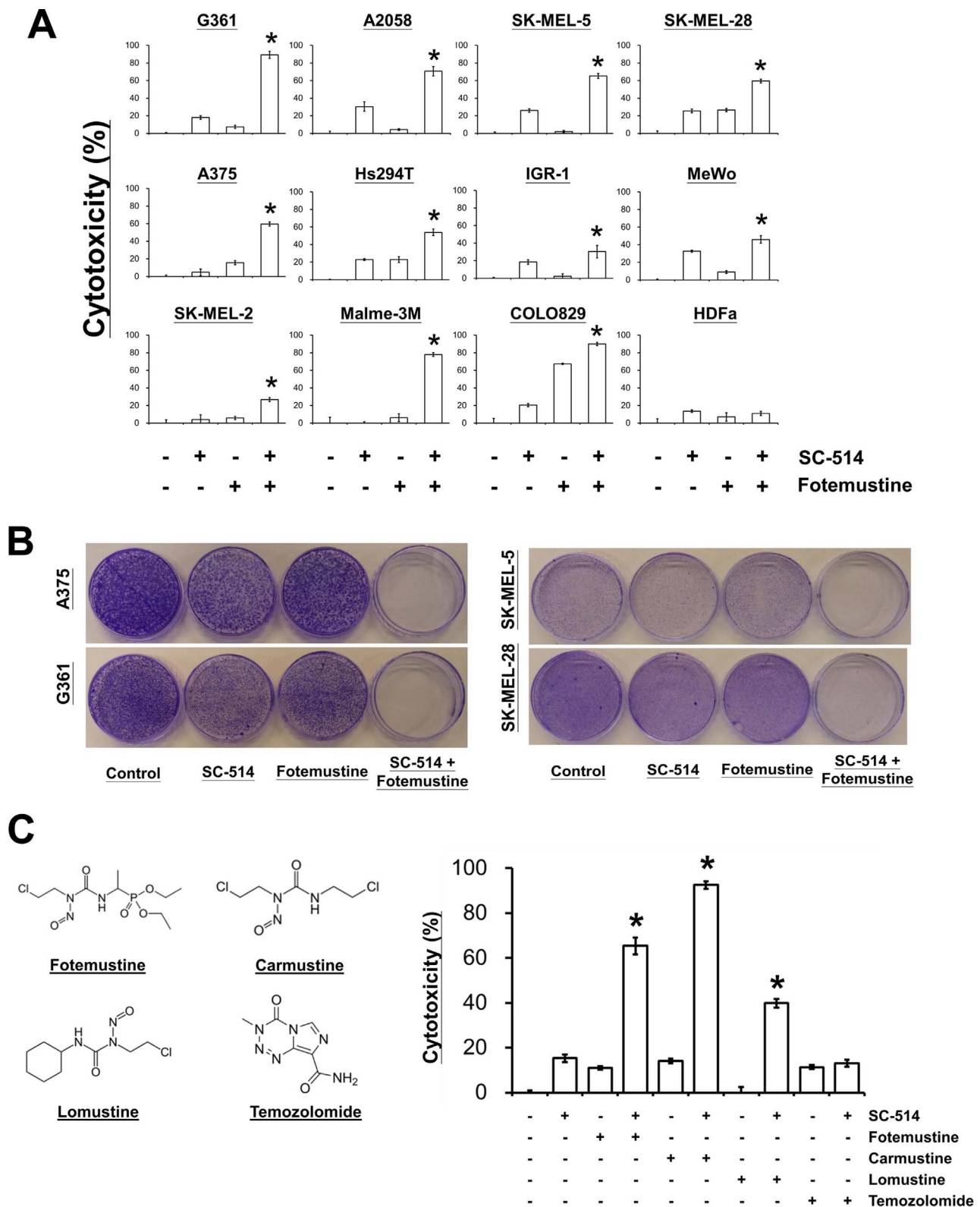


**Fig. 3.** SC-514 Sensitizes Nitrosourea-induced Melanoma Cell Death. (A) Indicated melanoma cell lines and normal human dermal fibroblasts adult (HDFa) were treated with vehicle or 50 μM SC-514 and/or 50 μM fotemustine for 2 days to determine the effect on proliferation. \*,  $p < 0.05$  versus control, SC-514 alone, and fotemustine alone. (B) Clonogenic survival assay of indicated melanoma cells treated with vehicle or 50 μM of SC-514 and/or 50 μM of fotemustine for 7 days. (C) Left, Chemical structure of four alkylating agents. Right, cell viability assay of G361 cells treated with vehicle or 50 μM of SC-514 and/or fotemustine (50 μM), carmustine (50 μM), lomustine (50 μM), temozolomide (100 μM) for 2 days. \*,  $p < 0.05$  versus control, SC-514 alone, and nitrosoureas alone. (D) Left, cell viability assay of parental and PLX4032-resistant A375 and G361 cells treated with 1 μM of PLX4032 for 2 days. Right, cell viability assay of PLX4032-resistant A375-R and G361-R cells treated with vehicle or 50 μM of SC-514 and/or 50 μM fotemustine for 2 days. \*,  $p < 0.05$  versus control, SC-514 alone, and fotemustine alone. (E) After transfection with control or catalase siRNAs for 24 h, A375 and G361 cells were treated with vehicle or 2.5 μM BMS-345541, 20 μM PS-1145 and/or 50 μM of fotemustine for an additional 48 h. Cell viability was then assessed. \*,  $p < 0.05$ . (F) A375 and G361 cells were treated with vehicle or 2.5 μM BMS-345541, 20 μM PS-1145 and/or 50 μM of fotemustine, in the presence or absence of catalase inhibitor 3-Amino-1,2,4-triazole (ATZ, 50 μM) for 48 h. Cell viability was then assessed. \*,  $p < 0.05$ .

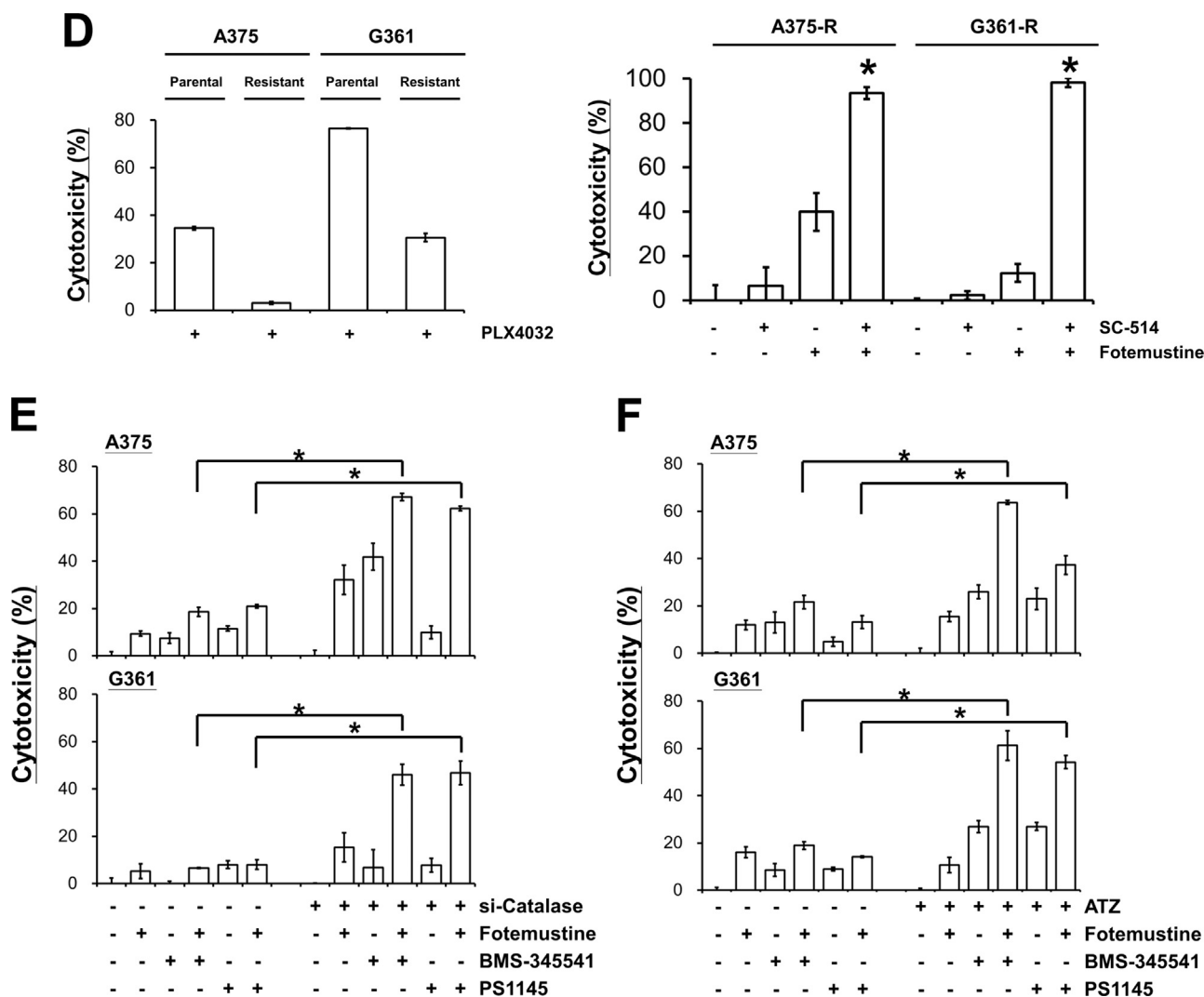


Fig. 3. (continued)

and G361 cells, while increase in phosphorylation of Chk2 at Thr68 was only observed in A375 cells, but not in G361 cells, under SC-514/fotemustine treatment (Fig. 4B).

To examine the capacity of SC-514 and/or fotemustine treatment to induce apoptosis in A375 and G361 melanoma cells, PARP/Caspase-3 cleavage analysis and flow cytometry assessment of Annexin V and propidium iodide staining were performed. We observed that the combination of SC-514/fotemustine induced reliable detection of apoptosis (Fig. 4C and Supplementary Fig. S3A). We also examined whether SC514/fotemustine would modulate the cell survival and apoptosis-related proteins. We found that SC514/fotemustine combination down-regulated the expression of survivin but had no apparent effect on the expression of other anti-apoptotic and cell survival proteins (Supplementary Fig. S3B).

Melanoma cells apoptosis induced by fotemustine was shown to be accompanied by DNA double-strand break formation [31]. Therefore, we investigated whether the combination SC-514 and fotemustine might result in increased H2AX phosphorylation (S139) levels, which acts as indicator of DNA damage and double-strand breaks. We found that SC-514 or fotemustine alone showed no or little induction of p-H2AX levels but the SC-514/fotemustine combination exerted dramatic increase in p-H2AX levels, and the effects was in a time-dependent manner (Fig. 4D). We also detected the formation of p-H2AX foci in A375 and G361 cells under SC-514/fotemustine treatment (Fig. 4E). Taken together, these data indicate that SC-514

potentiates the fotemustine-induced DNA damage and DNA double strand break in human melanoma cells.

### 3.5. ROS induction is essential in SC-514/fotemustine-induced melanoma cell death

It has been reported that tumor cell death induced by nitrosourea can be altered by the increase of ROS production [20]. We have shown above that SC-514 is a ROS-inducing IKK $\beta$  inhibitor that can enhance nitrosourea-induced melanoma cell death. To further investigate the role and significance of the changes in ROS in SC-514/fotemustine-induced cell death, we firstly measured the effect of SC-514/fotemustine combination on the overall oxidation state of human melanoma cells. We showed that as expected, treatment of SC-514 alone increased ROS production, while fotemustine treatment alone did not induce ROS production in A375 and G361 cells (Fig. 5A). SC-514/fotemustine combination only slightly enhanced ROS production compared to SC-514 alone (Fig. 5A). We also found that SC514/fotemustine combination had no apparent effect on the expression of catalase, SOD1 and IKK $\beta$  protein levels (Supplementary Fig. S4A). In addition to this, we observed that SC-514/fotemustine combination did not increase the oxidative DNA damage byproducts (Supplementary Fig. S4B), 8-OHdG, which is a ubiquitous maker of oxidative stress.

Next, we determined whether SC-514-induced ROS was essential in the sensitization of fotemustine-induced cell death. To address this

question, we tested whether anti-oxidant NAC was able to rescue the SC-514/fotemustine-induced cell death. We found that pretreatment with NAC significantly blocked the synergistic cell death action induced by SC-514 and fotemustine (Fig. 5B). We also showed that over-expression of catalase rescued the SC514/fotemustine-induced melanoma cell death (Supplementary Fig. S4C). Moreover, scavenging of ROS diminished the SC-514/fotemustine-induced p-H2AX, p-p53 and p53 levels (Fig. 5C). These results indicate that ROS induction is essential in SC-514/fotemustine-induced cell death.

Nitrosourea alkylating agents and fotemustine can induce DNA interstrand crosslink (ICL), which in turn impair DNA replication and transcription by preventing DNA strand separation, and leading to cancer cell death [8,9]. Recently studies demonstrated that the cytotoxicity of alkylating reagents can be enhanced by ROS with the effects of enhanced DNA crosslink levels and deleterious DNA damages (e.g., ICL formation or alkylation) [32–36]. Therefore, we further tested whether ROS would alter the DNA crosslink induced by nitrosoureas. To determine whether ROS would alter DNA crosslink in vitro, we analyzed the nitrosoureas-induced calf thymus DNA crosslink formation in the presence or absence of H<sub>2</sub>O<sub>2</sub>. This assay is based on the effect of snap cooling causes thermally denatured

covalently cross-linked DNA to rapidly renature, yielding fluorescence signals with H33258 dye; whereas, DNA lacking cross-links does not. H<sub>2</sub>O<sub>2</sub> alone caused slightly increase in DNA crosslink fraction (Fig. 5D). Treatment with various nitrosoureas (fotemustine, carmustine, lomustine) alone did induce ~10% of calf thymus DNA crosslink formation. However, when the calf thymus DNA was exposed to nitrosoureas together with H<sub>2</sub>O<sub>2</sub>, the DNA-crosslinked fraction increased to ~20% (Fig. 5D). Interestingly, H<sub>2</sub>O<sub>2</sub> did not alter the DNA-crosslink ability of another alkylating agent temozolomide.

The modified alkaline comet assay was used to measure DNA crosslink formation after fotemustine treatment in human melanoma cells. Analysis of ICL formation by the modified alkaline comet assay is based on the fact that ICL formation reduces DNA migration and percentage of DNA in comet tail induced by in vitro DNA strand break treatment [37,38]. As shown in Fig. 5E, in vitro treatment of H<sub>2</sub>O<sub>2</sub> induced DNA migration and increased in the percentage of DNA in comet tail. Treatment with fotemustine alone slightly induced DNA crosslink formation. Co-treatment with SC-514 significantly enhanced DNA crosslink levels induced by fotemustine, as evidenced by the decrease in the percentage of DNA in comet tail. Moreover, treatment with anti-oxidant NAC significantly rescued the SC-514/fotemustine-induced

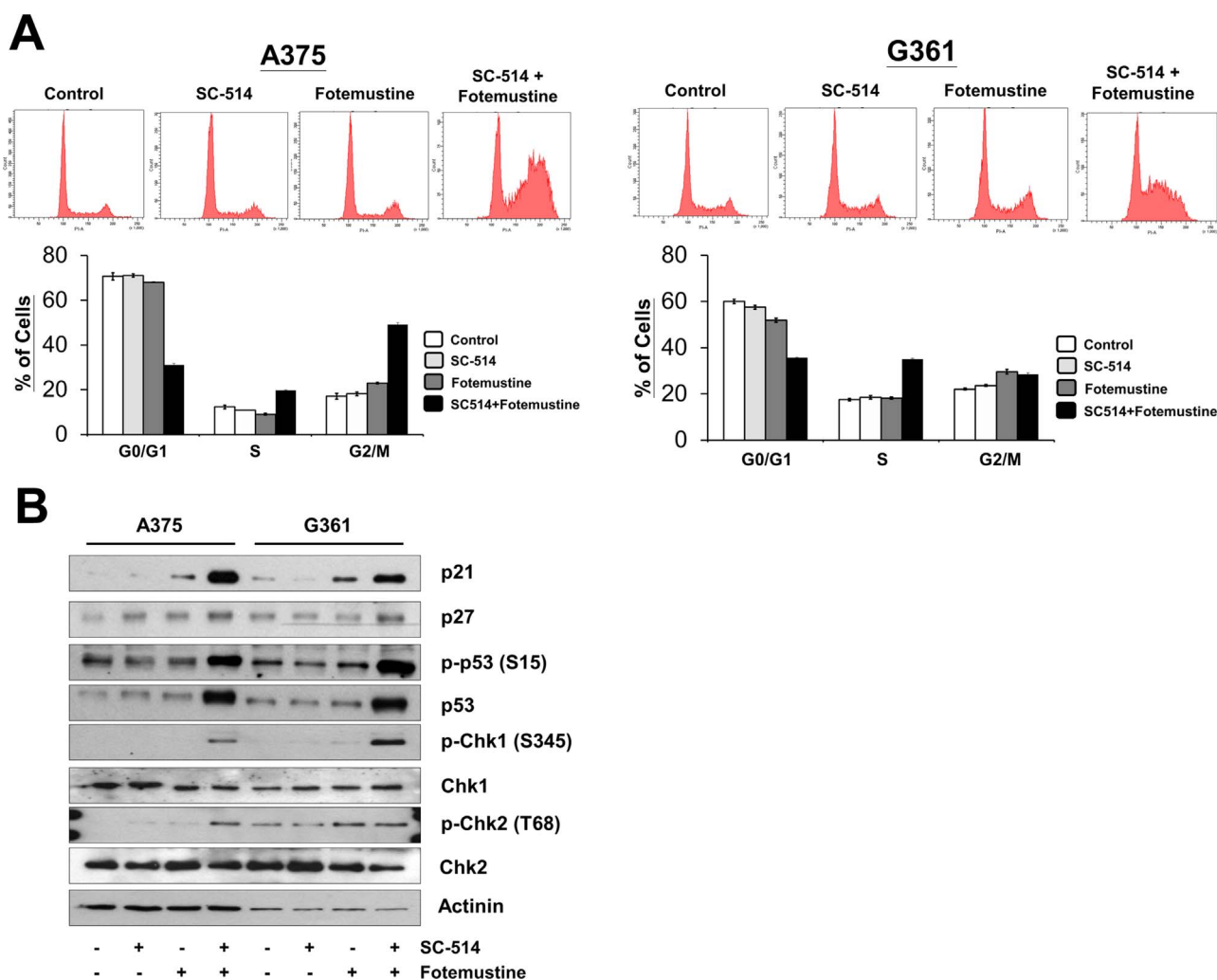


**Fig. 4.** SC-514/Fotemustine Combination Induces Concomitant DNA Damage, Cell Cycle Arrest and Apoptosis. (A) A375 and G361 melanoma cells were treated with vehicle or 50  $\mu$ M of SC-514 and/or 50  $\mu$ M of fotemustine for 24 h. The cell cycle phases of the treated cells were evaluated by flow cytometry. Data (% of cells) were expressed as mean  $\pm$  SD (n=3). (B) Indicated cells were exposed during 24 h to vehicle or 50  $\mu$ M of SC-514 and/or 50  $\mu$ M of fotemustine. Lysates were analyzed by Western Blotting using indicated antibodies. Results were representative of 3 independent experiments. (C) A375 and G361 cells were treated with vehicle or 50  $\mu$ M of SC-514 and/or 50  $\mu$ M of fotemustine for 36 h. Lysates were analyzed by Western Blotting using PARP and Caspase-3 antibodies. Results were representative of 3 independent experiments. (D) Indicated cells were exposed during 24 h or different time intervals (0,4,8,16 h) to vehicle or 50  $\mu$ M of SC-514 and/or 50  $\mu$ M of fotemustine. Lysates were analyzed by Western Blotting using p-H2AX(S139) and H2AX antibodies. Results were representative of 3 independent experiments. (E) Immunofluorescence staining showing a representative field of pH2AX-positive cells in indicated cells exposed 24 h to vehicle or 50  $\mu$ M of SC-514 and/or 50  $\mu$ M of fotemustine.

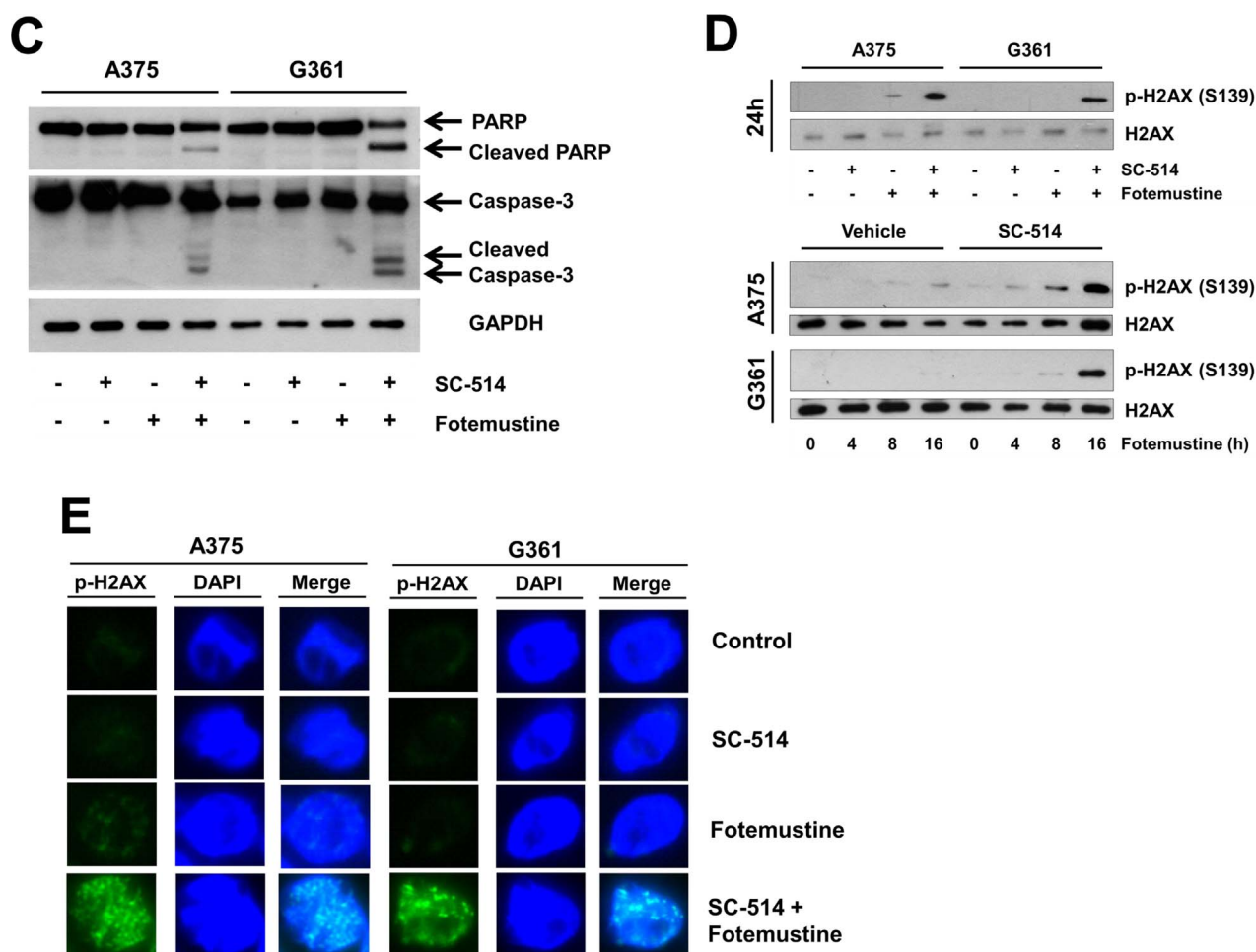


Fig. 4. (continued)

DNA crosslink, suggesting that the increase in DNA crosslink was triggered by ROS. Taken together, these data indicate that ROS can enhance nitrosoureas-induced DNA crosslink.

### 3.6. Overexpression of constitutively active IKK $\beta$ rescued SC-514/fotemustine-mediated DNA damage and cell death

Increasing evidence suggests that activation of the IKK $\beta$ -NF- $\kappa$ B pathway plays a key role in the development of cancer resistance to ionizing radiation and chemotherapy by promotion of DNA repair [16–18]. To determine the role of the changes of IKK $\beta$ -NF- $\kappa$ B pathway in SC-514/fotemustine-induced cell death, we firstly measured the effect of SC-514/fotemustine combination on the NF- $\kappa$ B activity of human melanoma cells. We found that as expected, treatment of SC-514 alone down-regulated NF- $\kappa$ B activity, while fotemustine treatment alone did not alter NF- $\kappa$ B activity in G361 cells (Fig. 6A). Combination of SC-514 and fotemustine resulted in enhanced NF- $\kappa$ B activity compared to SC-514 alone, but it was still slightly lower than the control (Fig. 6A), probably due to the activation of DNA damage-induced NF- $\kappa$ B signaling.

To validate the requirement of IKK $\beta$  inhibition in the enhanced DNA damage and cytotoxicity induced by fotemustine, constitutively active IKK $\beta$  (IKK $\beta$ -SS/EE), which was resistant to SC-514 inhibition (Supplementary Fig. S5), was expressed in human melanoma cells. We observed that SC-514/fotemustine-mediated H2AX phosphorylation

and cytotoxicity were attenuated in ectopic IKK $\beta$ -SS/EE-expressing A375 and G361 cells (Fig. 6, B and C). These results indicate that the enhancing effects by SC-514 were dependent on the inhibition of IKK $\beta$  activity. Previously studies suggested that the IKK $\beta$  can promote DNA repair by phosphorylating Ataxia-telangiectasia mutated (ATM) in response to DNA damage by alkylating agents [16]. We found that fotemustine alone stimulated ATM phosphorylation in a time-dependent manner in A375 and G361 cells while co-treatment with SC-514 diminished fotemustine-induced ATM phosphorylation (Fig. 6D). Overall, these findings suggest that inhibition of IKK $\beta$  activity is important in the synergistic effects between SC-514 and fotemustine.

O6-methylguanine-DNA methyltransferase (MGMT) is a DNA repair protein that has been shown previously to inhibit the lethal DNA cross-linking and induce resistance to alkylating agents including fotemustine [39–41]. We wondered whether melanoma cells that have high levels of MGMT would be still sensitized to fotemustine-induced cell death upon the challenge with ROS-inducing IKK $\beta$  inhibitor. To address this question, we over-expressed MGMT in human G361 melanoma cells and tested the SC-514/fotemustine-induced cytotoxicity. We found that ectopic expression of MGMT blocked the cytotoxic effects induced by SC-514 and fotemustine alone while had no effect on SC-514/fotemustine combination (Fig. 6E). These results indicate that the synergistic effects between fotemustine and SC-514 is probably relevant to different melanoma cells regardless of their basal MGMT content.

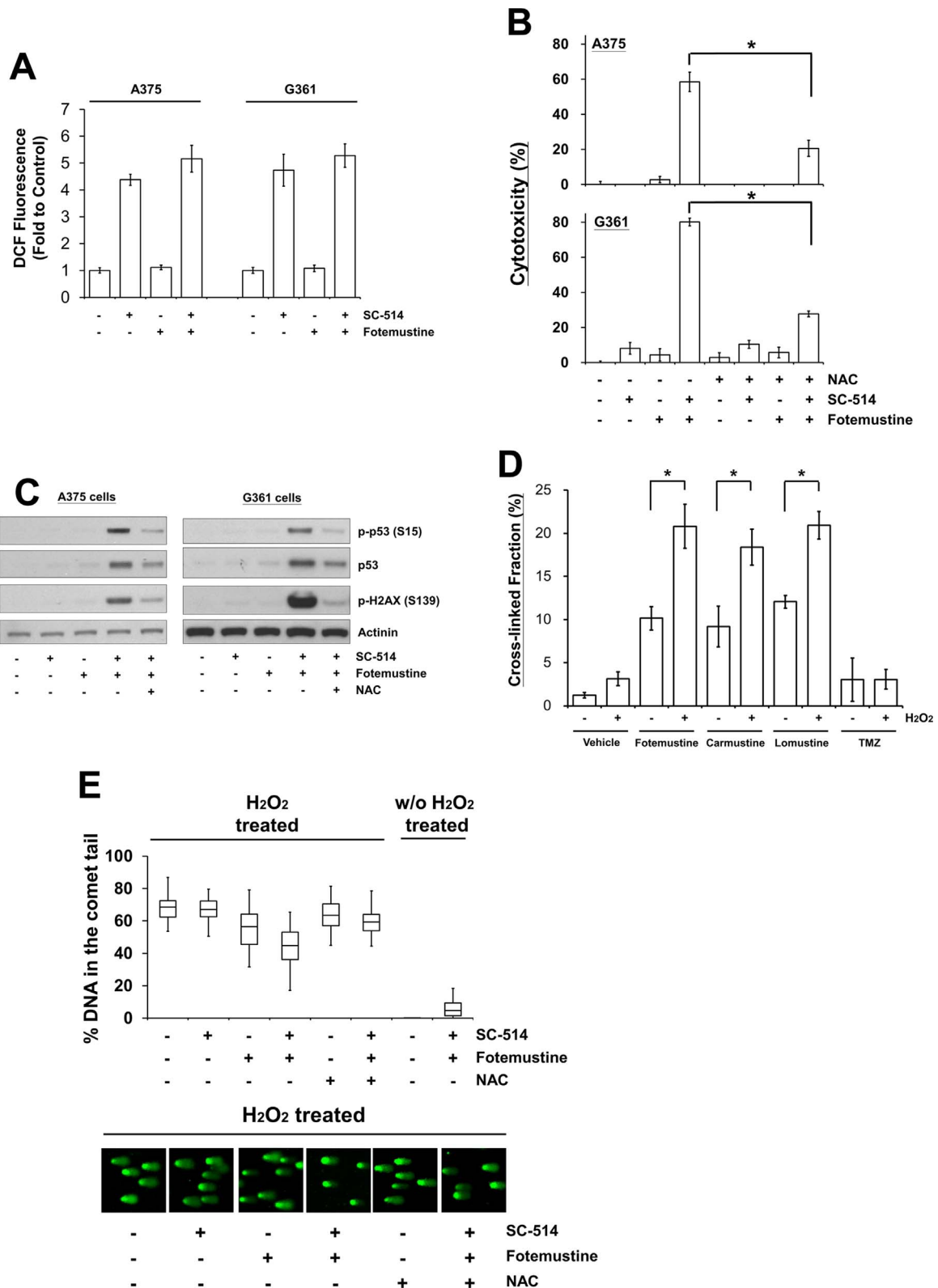


**Fig. 5.** ROS mediates SC-514/fotemustine-induced Cell death in Melanoma Cells. (A) A375 and G361 cells were loaded with 10  $\mu$ M DCF and further stimulated with vehicle or 50  $\mu$ M of SC-514 and/or 50  $\mu$ M of fotemustine for 3 h. Fluorescence was measured using a fluorescence microplate reader. (B) A375 and G361 cells were pretreated with vehicle or 5 mM NAC for 1 h, and then cells were further treated with 50  $\mu$ M of SC-514 and/or 50  $\mu$ M of fotemustine for additional 48 h. Cell viability was then assessed. \*,  $p < 0.05$ . (C) Indicated cells were exposed to vehicle or 50  $\mu$ M of SC-514 and/or 50  $\mu$ M of fotemustine with or without pretreatment of 5 mM NAC for 1 h. Lysates were analyzed by Western Blotting using indicated antibodies. Results were representative of 3 independent experiments. (D) Calf thymus DNA exposed to fotemustine (1 mM), carmustine (1 mM), lomustine (1 mM), temozolomide (TMZ, 1 mM) with or without 2 mM H<sub>2</sub>O<sub>2</sub> for 16 h. In vitro DNA crosslink assay was performed as described in Experimental Procedures section. Data (% of cross-linked fraction) were expressed as mean  $\pm$  SD (n=3). \*,  $p < 0.05$ . (E) Top, A375 cells were co-treated with 50  $\mu$ M of SC-514 and/or 50  $\mu$ M of fotemustine for 4 h, with or without pretreatment of 5 mM NAC for 1 h. Then, the percentage of DNA in comet tail was determined by modified alkaline comet assay and expressed in box and whisker plot. Bottom, representative images of modified alkaline comets.

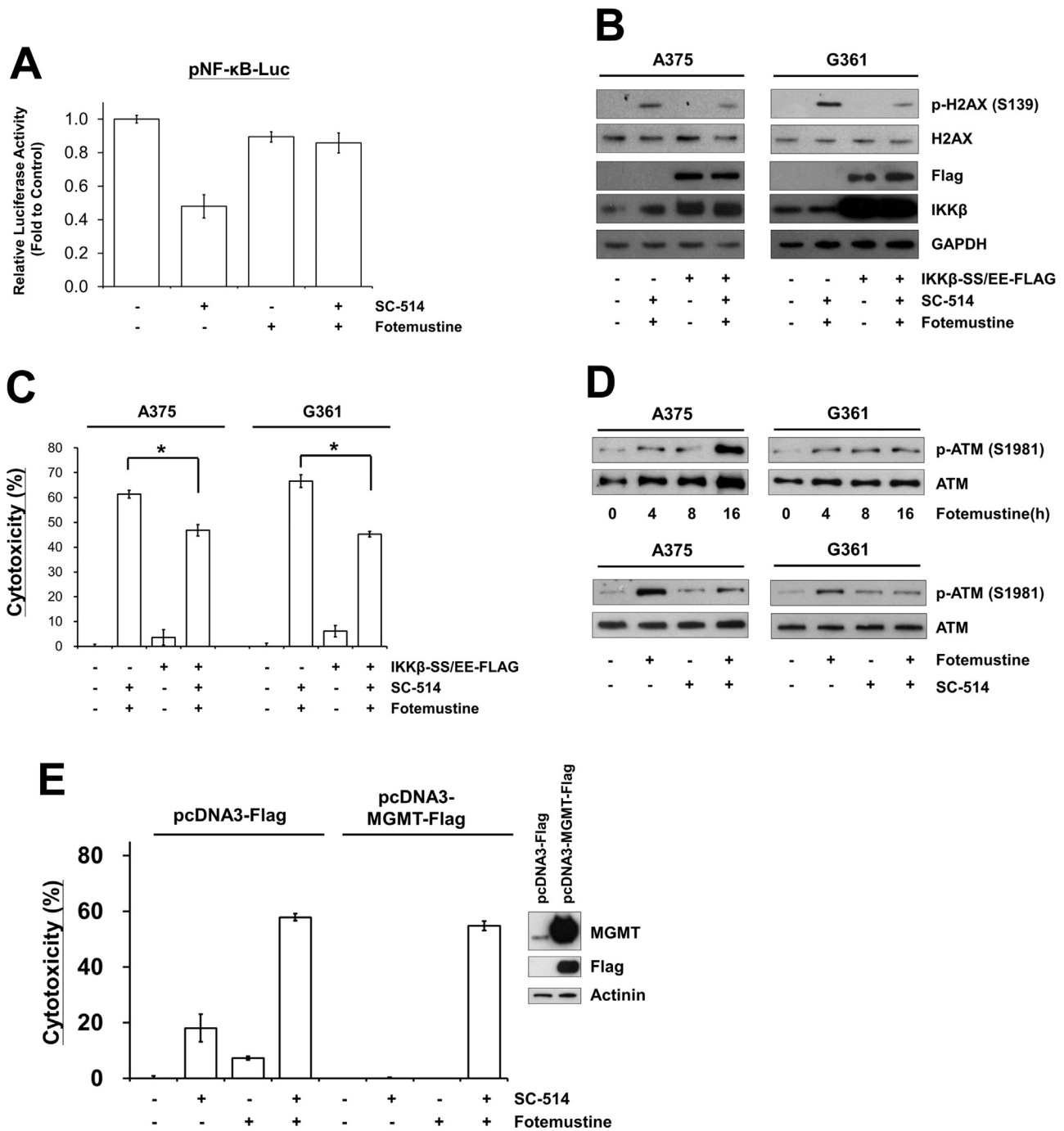
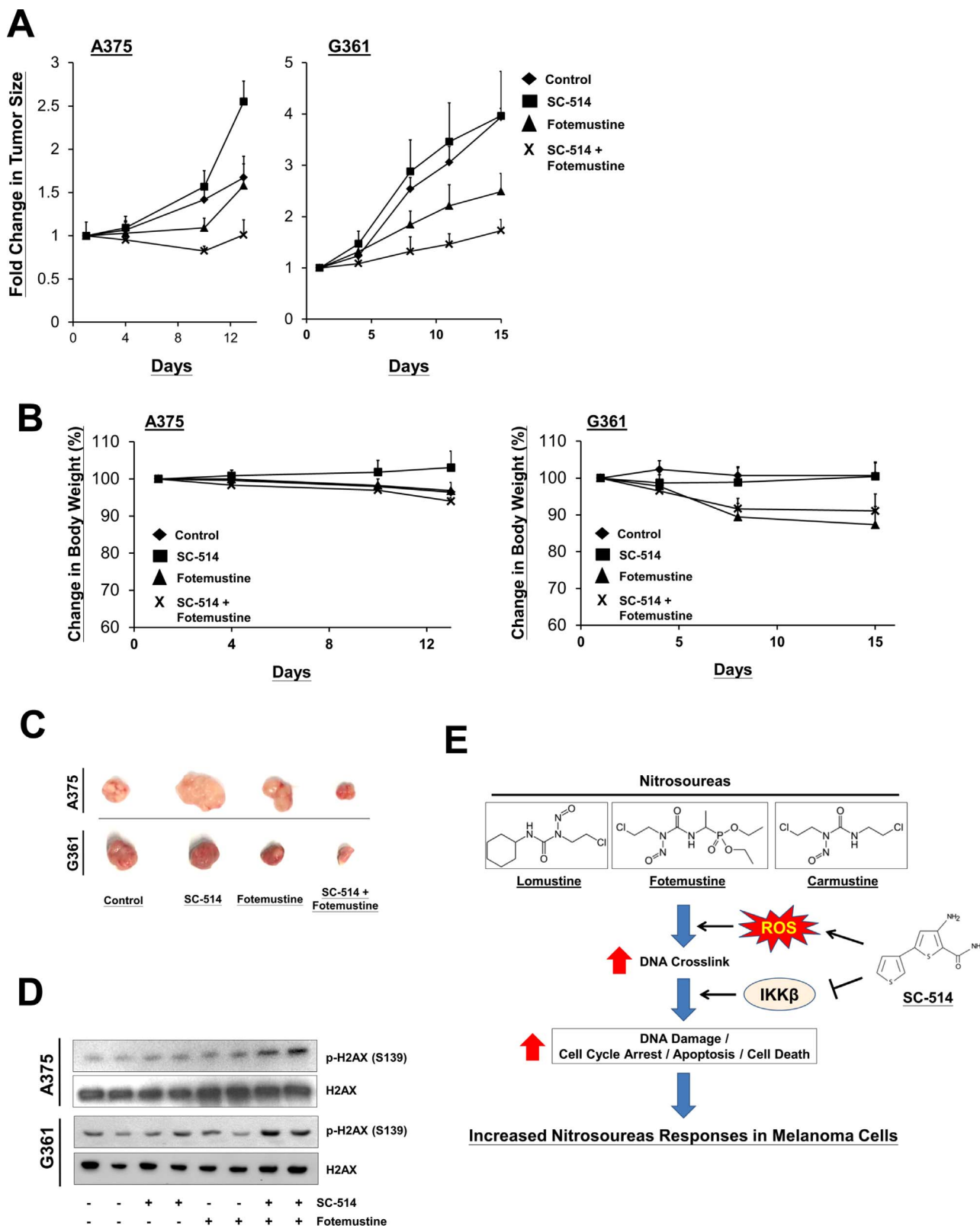


**Fig. 6.** Overexpression of constitutively active IKKβ rescued SC-514/fotemustine-mediated DNA Damage and Cell Death. (A) Luciferase activity of G361 cells transfected with pNF-κB-Luc and treated with vehicle or 50 μM of SC-514 and/or 50 μM of fotemustine for 24 h. At least two independent experiments with triplicates revealed comparable results. (B) After transfection with constitutively active IKKβ (IKKβ-SS/EE-FLAG) for 24 h, A375 and G361 cells were treated with vehicle or 50 μM of SC-514 and/or 50 μM of fotemustine for additional 24 h. Western blotting analysis of constitutively active IKKβ (IKKβ-SS/EE-FLAG) transfected G361 cells using p-H2AX, H2AX, Flag, IKKβ and GAPDH antibodies was shown. (C) After transfection with constitutively active IKKβ (IKKβ-SS/EE-FLAG) for 24 h, A375 and G361 cells were treated with vehicle or 50 μM of SC-514 and/or 50 μM of fotemustine for an additional 48 h. Cell viability was then assessed. \*,  $p < 0.05$ . (D) Upper, Indicated cells were exposed to vehicle or 50 μM of fotemustine for different time intervals (h). Bottom, Indicated cells were exposed to vehicle or 50 μM of SC-514 and/or 50 μM of fotemustine for 16 h (A375) and 4 h (G361). Lysates were analyzed by Western Blotting using indicated antibodies. (E) After transfection with MGMT expression vector for 24 h, G361 cells were treated with vehicle or 50 μM of SC-514 and/or 50 μM of fotemustine for an additional 48 h. Cell viability was then assessed. \*,  $p < 0.05$ . Western blot analysis of MGMT and FLAG from transfected G361 cells lysates is also shown.

**3.7. SC-514 cooperates with fotemustine to inhibit melanoma development in vivo**

To obtain in vivo evidence for the implication of SC-514 in the response of cancer cells to fotemustine, we used the xenograft mouse model of melanoma. Nude mice engrafted with A375 or G361 tumors were treated with vehicle control and 25 mg/kg SC-514 and/or 25 mg/kg

25 mg/kg fotemustine daily for 13–15 consecutive days and the tumor behavior was monitored. In agreement with our observations in vitro melanoma cell lines studies, fotemustine treatment with SC-514 showed a clear combined effect and reduced the size of tumors in mice (Fig. 7, A and C). Fotemustine treatment alone caused reduction in body weight and their combination with SC-514 exerted either no change (A375-bearing mice) or slightly rescued the body weight



reduction (G361-bearing mice) (Fig. 7B). Consistent with the results in human melanoma cell lines, SC-514 increased fotemustine-induced DNA damage signaling, represented by enhanced p-H2AX levels, in the A375 and G361 tumors (Fig. 7D).

#### 4. Discussion

Nitrosourea is considered as an active agent in the treatment of melanoma brain metastases and glioma because it has remarkable ability to cross the blood–brain barrier [10,11]. However, a considerable number of cancer cell types are highly resistant to nitrosourea treatment due to the high level of DNA repair protein expression [39–41]. Moreover, the non-specific toxicity induced by nitrosourea causes serious side effects and hampers its clinical use. Therefore, novel therapeutic strategies to enhance nitrosourea-induced cytotoxicity without causing serious side effects are urgently needed to overcome problems of using nitrosourea clinically. In this study, we demonstrate for the first time that SC-514, a ROS-inducing IKK $\beta$  inhibitor, effectively sensitized human melanoma cells to nitrosourea-induced cell death. SC-514 induced ROS which mediated the enhancement of DNA crosslink induced by fotemustine and inhibition of IKK $\beta$  activity by SC-514 potentiated DNA damage responses (summarized in Fig. 7E). Most importantly, no enhancement in cytotoxicity by SC-514/fotemustine was observed in normal human adult dermal fibroblast cells (HDFa) (Fig. 3A) and the synergistic effects between SC-514 and fotemustine did not cause further body weight reduction compared with fotemustine treatment alone (Fig. 7B). Therefore, the combination of ROS-inducing IKK $\beta$  inhibitor and nitrosourea may be an effective cancer therapy that warrants additional study in future.

Nitrosourea alkylating agents, including fotemustine, carmustine and lomustine, induce DNA interstrand cross-linking, and lead to improper DNA replication and cell death [8,9]. Previous studies reported that the DNA crosslink ability of alkylating agent could be altered by ROS. Several peroxidases, such as horseradish peroxidase, myeloperoxidase, and lactoperoxidase, were found to oxidize mitomycin C hydroquinone to mitomycin C and therefore block DNA cross-linking [42]. On the other hand, recently studies showed that the cytotoxicity of alkylating reagents can be enhanced by ROS, by formation of ROS-activated prodrugs resulting in higher DNA crosslink activity. Peng's group revealed that the prodrugs of nitrogen mustard coupled with an ROS trigger unit can be triggered by H<sub>2</sub>O<sub>2</sub> to release active anticancer drugs with higher DNA crosslink activities, leading to selective toxicity toward primary leukemic lymphocytes but less toxic to normal lymphocytes [32–36]. In this study, we found that ROS induced by SC-514 enhanced nitrosourea-induced DNA crosslink and cytotoxicity (Fig. 4, D and E). To our best knowledge, this is the first example to show the DNA crosslink activity of nitrosourea can be activated by ROS. We also showed that the SC-514/fotemustine combination gave no synergistic cytotoxicity in normal human dermal fibroblast (Fig. 3A). Although our findings are promising, further work is needed to clarify whether ROS will activate the DNA crosslink ability of nitrosourea by the formation of activated nitrosourea derivatives.

Previous studies showed that the inducible DNA crosslink activity from nitrogen mustard prodrug could be differentially triggered by various ROS such as hydrogen peroxide (H<sub>2</sub>O<sub>2</sub>), tertbutylhydroperoxide (TBHP), hypochlorite (OCl<sup>-</sup>), hydroxyl radical (HO<sup>•</sup>), tert-butoxy radical (BuO<sup>•</sup>), superoxide (O<sub>2</sub><sup>-</sup>), and nitric oxide (NO) [33,35]. In this study, we found that addition of H<sub>2</sub>O<sub>2</sub> increased the nitrosourea-induced DNA crosslink in vitro (Fig. 5D) and simultaneous treatment with IKK $\beta$  and catalase siRNA resulted in synergistic increases in growth inhibition induced by fotemustine in both A375 and G361 cells (Fig. 1, A and B). We also observed that simultaneous treatment with IKK $\beta$  and SOD1 siRNA resulted in increase in growth inhibition induced by fotemustine (Supplementary Fig. S1). Further studies are, however, needed to determine the possible involvement of other ROS in the activation of nitrosoureas. We demonstrated that SC-514 was not

able to enhance the cytotoxic effect of monofunctional alkylating temozolomide (Fig. 3C). This phenomenon can be explained by the fact that H<sub>2</sub>O<sub>2</sub> could not alter the DNA-crosslink ability of temozolomide (Fig. 5D) but needed to be verified and further investigated in future. In this study, the oxidative DNA damage (8-OHdG) could not be detected in SC-514/fotemustine treated cells (Supplementary Fig. S4B). These results indicated that ROS produced by SC-514 alone or SC-514/fotemustine combination were not sufficient for inducing oxidative DNA damage but could only enhanced DNA-crosslink ability of fotemustine.

Our results indicated that ROS-inducing IKK $\beta$  inhibitor SC-514 enhanced nitrosourea-induced cell death in melanoma cells. SC-514 has been reported to be a selective IKK $\beta$  inhibitor and was > 10-fold selectivity against 28 other kinases, including both tyrosine kinases and other serine- threonine kinases [43]. In the current study, we observed that SC-514 is the only compound with the ROS-inducing property among the IKK $\beta$  inhibitors we tested. The mechanism of how SC-514 could induce H<sub>2</sub>O<sub>2</sub>/ROS is unknown. We showed that SC-514 did not alter the catalase or SOD1 expression in melanoma cells (Supplementary Fig. S4A). Recent studies suggested that mitochondria-targeting molecules can lead to the release of cellular ROS [44]. Therefore, further work is needed to clarify whether SC-514 will induce ROS by the attacking mitochondrial components. As ROS-inducing IKK $\beta$  inhibitor was shown to effectively enhance nitrosourea-induced melanoma cell death, it is interesting to explore if there is other ROS-inducing IKK $\beta$  inhibitor, by a large scale and high throughput screening. Alternatively, ROS-inducing IKK $\beta$  inhibitor can be synthesized based on chemical approach, with the goal of providing safe and effective treatment regimens for melanoma. On the other hand, some IKK $\beta$  inhibitors such as AZD3264 (Fig. 2C) and wedelolactone (data not shown) are antioxidant. Thus, it is crucial to consider the overall cellular redox potential in the future clinical use of combination of IKK $\beta$  and nitrosourea, in order to prevent the potential antagonistic effects. Interestingly, SC-514 treatment alone was found to increase A375 but not G361 tumor progression in xenograft nude mice model (Fig. 7A). Increasing evidences suggest that high ROS levels contribute to melanoma progression [45,46], which may account for the action of SC-514 on A375 xenograft. Nevertheless, the ROS-inducing IKK $\beta$  inhibitor/fotemustine combination showed a clear combined effect and reduced the size of A375 and G361 tumors in mice (Fig. 7, A and C) that warrants additional study in future.

Previous reports have shown that inhibition of IKK $\beta$  can promote DNA repair by phosphorylates nuclear ATM in response to DNA damage by alkylating agents [16]. We showed that SC-514 inhibited the fotemustine-induced ATM phosphorylation (Fig. 6D). The detailed mechanisms of how SC-514 inhibits the fotemustine-induced ATM phosphorylation need to be further investigated. SC-514 has been shown to be a selective and competitive inhibitor of the ATP site of activated IKK $\beta$  [43]. Therefore, further experiments are needed to show whether SC-514 will block the IKK $\beta$ -ATM enzyme substrate reaction. Sakamoto et al. [16] revealed that activated IKK $\beta$  generated during the DNA damage response was found to translocate into the nucleus and directly phosphorylate ATM. We observed that combination of SC-514 and fotemustine resulted in enhanced NF- $\kappa$ B activity compared to SC-514 alone (Fig. 6A) without affecting the IKK $\beta$  nuclear translocation in melanoma cells (data not shown), indicating that SC-514 may alter the ATM phosphorylation by lowering the IKK $\beta$  kinase activity.

Nitrosourea-induced anti-tumor effects in malignant melanoma are limited by direct repair of O<sub>6</sub>-alkyl groups by MGMT [39–41]. In our study, SC-514 significantly enhanced fotemustine-induced cytotoxicity in all melanoma cell lines tested (Fig. 3A). We found that ectopic expression of MGMT had no effect on SC-514/fotemustine combination (Fig. 6E). In addition, we have performed MGMT expression profiling study and found that there are differential levels of MGMT expressed in different melanoma cell lines, with a highest MGMT gene

expression in G361 cells (Supplementary Fig. S6). Taken together, the synergistic effects between fotemustine and SC-514 is probably relevant to different melanoma cells regardless of their basal MGMT content and therefore provides a broadly application basis for its clinically use for treating melanoma. Besides MGMT repair pathway, the Mre11-Rad50-Nbs1 (MRN) complex is involved in DNA damage detection and signaling [47] and contributes to the control of alkylating agent-induced cell cycle arrest and cytotoxicity [48]. We found that SC-514/fotemustine combination did not alter the expression of MRN complex (Supplementary Fig. S7). With the addition of MRN inhibitor mirin [49], the SC-514/fotemustine-induced cytotoxicity was further enhanced (Supplementary Fig. S7). These findings indicated that blockage of other DNA repair pathway may further augment the cytotoxic effects induced by the combination of a ROS-inducing IKK $\beta$  inhibitor and nitrosourea.

In summary, our results illustrate a new drug synergism strategy to enhance the effect of nitrosourea by combining a ROS-inducing IKK $\beta$  inhibitor, and shed new lights on the scientific basis on the clinical use of ROS-inducing IKK $\beta$  inhibitors as sensitizers for alkylating agents treatment for melanoma. ROS generated by SC-514 plays a critical role in DNA crosslink upregulation, and inhibition of IKK $\beta$  signaling pathways is important for the enhancement of DNA damage signaling. As nitrosourea is used clinically, further clinical studies are warranted to explore the combined effects of ROS-inducing IKK $\beta$  inhibitors and nitrosourea, with the goal of providing safe and effective treatment regimens for melanoma.

#### Disclosure of potential conflicts of interest

No potential conflicts of interest were disclosed.

#### Acknowledgments

We thank the technical staffs in School of Chinese Medicine-Hong Kong Baptist University for expertise in all experiments. This work was partially supported by Food and Health Bureau of Hong Kong (HMRP 11122441), Hong Kong Baptist University (FRG2/13–14/046 and FRG2/14–15/104), National Natural Science Foundation of China (81673649), Science, Technology and Innovation Commission of Shenzhen (JCYJ20140807091945050, JCYJ20150630164505508 and JCYJ20160229210327924); Research Grants Council of Hong Kong (12125116); Guangdong Natural Science Foundation (2016A030313007); and Consun Pharmaceutical Group Limited.

#### Appendix A. Supporting material

Supplementary data associated with this article can be found in the online version at doi:10.1016/j.redox.2017.01.010.

#### References

- [1] D.L. Cummins, J.M. Cummins, H. Pantle, M.A. Silverman, A.L. Leonard, A. Chanmugam, Cutaneous malignant melanoma, *Mayo Clin. Proc.* 81 (2006) 500–507.
- [2] L. Finn, S.N. Markovic, R.W. Joseph, Therapy for metastatic melanoma: the past, present, and future, *BMC Med.* 10 (2012) 23.
- [3] Z. Zhu, W. Liu, V. Gotlieb, The rapidly evolving therapies for advanced melanoma – towards immunotherapy, molecular targeted therapy, and beyond, *Crit. Rev. Oncol. Hematol.* 99 (2016) 91–99.
- [4] S. Puyo, D. Montaudon, P. Pourquier, From old alkylating agents to new minor groove binders, *Crit. Rev. Oncol. Hematol.* 89 (2014) 43–61.
- [5] R.J. Davey, A. van der Westhuizen, N.A. Bowden, Metastatic melanoma treatment: combining old and new therapies, *Crit. Rev. Oncol. Hematol.* 98 (2016) 242–253.
- [6] D.M. Palathinkal, T.R. Sharma, H.B. Koon, J.S. Bordeaux, Current systemic therapies for melanoma, *Dermatol. Surg.* 40 (2014) 948–963.
- [7] P. Beauchesne, Fotemustine: a third-generation nitrosourea for the treatment of recurrent malignant gliomas, *Cancers* 4 (2012) 77–87.
- [8] D. Fu, J.A. Calvo, L.D. Samson, Balancing repair and tolerance of DNA damage caused by alkylating agents, *Nat. Rev. Cancer* 12 (2012) 104–120.
- [9] M.T. Hayes, J. Bartley, P.G. Parsons, G.K. Eaglesham, A.S. Prakash, Mechanism of action of fotemustine, a new chloroethylnitrosourea anticancer agent: evidence for the formation of two DNA-reactive intermediates contributing to cytotoxicity, *Biochemistry* 36 (1997) 10646–10654.
- [10] D. Khayat, B. Giroux, J. Berille, V. Cour, B. Gerard, M. Sarkany, et al., Fotemustine in the treatment of brain primary tumors and metastases, *Cancer Invest.* 12 (1994) 414–420.
- [11] G. Quéreux, B. Dréno, Fotemustine for the treatment of melanoma, *Expert Opin. Pharm.* 12 (2011) 2891–2904.
- [12] M.F. Avril, S. Aamdal, J.J. Grob, A. Hauschild, P. Mohr, J.J. Bonerandi, et al., Fotemustine compared with dacarbazine in patients with disseminated malignant melanoma: a phase III study, *J. Clin. Oncol.* 22 (2004) 1118–1125.
- [13] T. Yamashima, J. Yamashita, K. Shoin, Neurotoxicity of local administration of two nitrosoureas in malignant gliomas, *Neurosurgery* 26 (1990) 794–799.
- [14] Z. Khalil, N. Pageot, B. Carlander, B. Guillot, Neurological toxicity during metastatic melanoma treatment with fotemustine, *Melanoma Res.* 15 (2005) 563–564.
- [15] J. Napetschnig, H. Wu, Molecular basis of NF- $\kappa$ B signaling, *Annu. Rev. Biophys.* 42 (2013) 443–468.
- [16] K. Sakamoto, Y. Hikiba, H. Nakagawa, Y. Hirata, Y. Hayakawa, H. Kinoshita, et al., Promotion of DNA repair by nuclear IKK $\beta$  phosphorylation of ATM in response to genotoxic stimuli, *Oncogene* 32 (2013) 1854–1862.
- [17] Z.H. Wu, Y. Shi, R.S. Tibbetts, S. Miyamoto, Molecular linkage between the kinase ATM and NF-kappaB signaling in response to genotoxic stimuli, *Science* 311 (2006) 1141–1146.
- [18] L. Wu, L. Shao, N. An, J. Wang, S. Pazhanisamy, W. Feng, et al., IKK $\beta$  regulates the repair of DNA double-strand breaks induced by ionizing radiation in MCF-7 breast cancer cells, *PLoS One* 6 (2011) e18447.
- [19] M. Valko, C.J. Rhodes, J. Moncol, M. Izakovic, M. Mazur, Free radicals, metals and antioxidants in oxidative stress-induced cancer, *Chem. Biol. Inter.* 160 (2006) 1–40.
- [20] C.C. Kuo, T.W. Liu, L.T. Chen, H.S. Shiah, C.M. Wu, Y.T. Cheng, et al., Combination of arsenic trioxide and BCNU synergistically triggers redox-mediated autophagic cell death in human solid tumors, *Free Radic. Biol. Med.* 51 (2011) 2195–2209.
- [21] F. Mercurio, H. Zhu, B.W. Murray, A. Shevchenko, B.L. Bennett, J. Li, et al., IKK-1 and IKK-2: cytokine-activated IkkappaB kinases essential for NF-kappaB activation, *Science* 278 (1997) 860–866.
- [22] A.K. Tse, H.H. Cao, C.Y. Cheng, H.Y. Kwan, H. Yu, W.F. Fong, et al., Indomethacin sensitizes TRAIL-resistant melanoma cells to TRAIL-induced apoptosis through ROS-mediated upregulation of death receptor 5 and downregulation of survivin, *J. Invest. Dermatol.* 134 (2014) 1397–1407.
- [23] A.K. Tse, C.K. Wan, X.L. Shen, M. Yang, W.F. Fong, Honokiol inhibits TNF- $\alpha$ -stimulated NF- $\kappa$ B activation and NF- $\kappa$ B-regulated gene expression through suppression of IKK activation, *Biochem. Pharm.* 70 (2005) 1443–1457.
- [24] Y. Yang, A.K. Tse, P. Li, Q. Ma, S. Xiang, S.V. Nicosia, et al., Inhibition of androgen receptor activity by histone deacetylase 4 through receptor Sumoylation, *Oncogene* 30 (2011) 2207–2218.
- [25] J. Wu, J. Du, X. Fu, B. Liu, H. Cao, T. Li, et al., Icartin, a novel FASN inhibitor, exerts anti-melanoma activities through IGF-1R/STAT3 signaling, *Oncotarget* 7 (32) (2016) 51251–51269.
- [26] J.M. Gasent Blesa, E. Grande Pulido, V. Alberola Candel, M. Provencio Pulla, Melanoma: from darkness to promise, *Am. J. Clin. Oncol.* 34 (2011) 179–187.
- [27] H. Davies, G.R. Bignell, C. Cox, P. Stephens, S. Edkins, S. Clegg, et al., Mutations of the BRAF gene in human cancer, *Nature* 417 (2002) 949–954.
- [28] P.B. Chapman, A. Hauschild, C. Robert, J.B. Haanen, P. Ascierto, J. Larkin, et al., Improved survival with vemurafenib in melanoma with BRAF V600E mutation, *N. Engl. J. Med.* 364 (2011) 2507–2516.
- [29] F. Spagnolo, P. Ghiorzo, L. Orgiano, L. Pastorino, V. Picasso, E. Tornari, et al., BRAF-mutant melanoma: treatment approaches, resistance mechanisms, and diagnostic strategies, *Onco Targets Ther.* 8 (2015) 157–168.
- [30] M.T. Hayes, J. Bartley, P.G. Parsons, In vitro evaluation of fotemustine as a potential agent for limb perfusion in melanoma, *Melanoma Res.* 8 (1998) 67–75.
- [31] S.C. Naumann, W.P. Roos, E. Jöst, C. Belohlavek, V. Lennerz, C.W. Schmidt, et al., Temozolomide- and fotemustine-induced apoptosis in human malignant melanoma cells: response related to MGMT, MMR, DSBs, and p53, *Br. J. Cancer* 100 (2009) 322–333.
- [32] S. Cao, Y. Wang, X. Peng, ROS-inducible DNA cross-linking agent as a new anticancer prodrug building block, *Chemistry* 18 (2012) 3850–3854.
- [33] W. Chen, K. Balakrishnan, Y. Kuang, Y. Han, M. Fu, V. Gandhi, et al., Reactive oxygen species (ROS) inducible DNA cross-linking agents and their effect on cancer cells and normal lymphocytes, *J. Med. Chem.* 57 (2014) 4498–4510.
- [34] W. Chen, Y. Han, X. Peng, Aromatic nitrogen mustard-based prodrugs: activity, selectivity, and the mechanism of DNA cross-linking, *Chemistry* 20 (2014) 7410–7418.
- [35] Y. Kuang, K. Balakrishnan, V. Gandhi, X. Peng, Hydrogen peroxide inducible DNA cross-linking agents: targeted anticancer prodrugs, *J. Am. Chem. Soc.* 133 (2011) 19278–19281.
- [36] G. Li, T. Bell, E.J. Merino, Oxidatively activated DNA-modifying agents for selective cytotoxicity, *ChemMedChem* 6 (2011) 869–875.
- [37] M. Volpato, J. Seargent, P.M. Loadman, R.M. Phillips, Formation of DNA interstrand cross-links as a marker of mitomycin C bioreductive activation and chemosensitivity, *Eur. J. Cancer* 41 (2005) 1331–1338.
- [38] J.H. Wu, N.J. Jones, Assessment of DNA interstrand crosslinks using the modified alkaline comet assay, *Methods Mol. Biol.* 817 (2012) 165–181.
- [39] M. Christmann, M. Pick, H. Lage, D. Schadendorf, B. Kaina, Acquired resistance of melanoma cells to the antineoplastic agent fotemustine is caused by reactivation of the DNA repair gene mgmt, *Int. J. Cancer* 92 (2001) 123–129.

- [40] I. Passagne, A. Evrard, J.Y. Winum, P. Depeille, P. Cuq, J.L. Montero, et al., Cytotoxicity, DNA damage, and apoptosis induced by new fotemustine analogs on human melanoma cells in relation to O6-methylguanine DNA-methyltransferase expression, *J. Pharm. Exp. Ther.* 307 (2003) 816–823.
- [41] Z. Wu, C.L. Chan, A. Eastman, E. Bresnick, Expression of human O6-methylguanine-DNA methyltransferase in chinese hamster ovary cells and restoration of cellular resistance to certain N-nitroso compounds, *Mol. Carcinog.* 4 (1991) 482–488.
- [42] P.G. Penketh, W.F. Hodnick, M.F. Belcourt, K. Shyam, D.H. Sherman, A.C. Sartorelli, Inhibition of DNA cross-linking by mitomycin C by peroxidase-mediated oxidation of mitomycin C hydroquinone, *J. Biol. Chem.* 276 (2001) 34445–34452.
- [43] N. Kishore, C. Sommers, S. Mathialagan, J. Guzova, M. Yao, S. Hauser, et al., A selective IKK-2 inhibitor blocks NF-kappa B-dependent gene expression in interleukin-1 beta-stimulated synovial fibroblasts, *J. Biol. Chem.* 278 (2003) 32861–32871.
- [44] J. Dan Dunn, L.A. Alvarez, X. Zhang, T. Soldati, Reactive Oxygen Species and Mitochondria: A nexus of cellular homeostasis, 6, 2015, pp.472–85.
- [45] A. Joosse, E. De Vries, C.H. van Eijck, A.M. Eggermont, T. Nijsten, J.W. Coebergh, Reactive oxygen species and melanoma: an explanation for gender differences in survival?, *Pigment Cell Melanoma Res.* 23 (2010) 352–364.
- [46] H.G. Wittgen, L.C. van Kempen, Reactive oxygen species in melanoma and its therapeutic implications, *Melanoma Res.* 17 (2007) 400–409.
- [47] G.J. Williams, S.P. Lees-Miller, J.A. Tainer, Mre11–Rad50–Nbs1 conformations and the control of sensing, signaling, and effector responses at DNA double-strand breaks, *DNA Repair* 9 (2010) 1299–1306.
- [48] O.K. Mirzoeva, T. Kawaguchi, R.O. Pieper, The Mre11/Rad50/Nbs1 complex interacts with the mismatch repair system and contributes to temozolomide-induced G2 arrest and cytotoxicity, *Mol. Cancer Ther.* 5 (2006) 2757–2766.
- [49] A. Dupré, L. Boyer-Chatenet, R.M. Sattler, A.P. Modi, J.H. Lee, M.L. Nicolette, et al., A forward chemical genetic screen reveals an inhibitor of the Mre11–Rad50–Nbs1 complex, *Nat. Chem. Biol.* 4 (2008) 119–125.